

Effect of Solvent Plasticization on Polypropylene Microcellular Foaming Process and Foam Characteristics

W. Kaewmesri,¹ P. Rachtanapun,² J. Pumchusak³

¹Department of Materials Science, Faculty of Science, Chiang Mai University, Muang, Chiang Mai 50200, Thailand

²Department of Packaging Technology, Faculty of Agro-Industry, Chiang Mai University, Mae-Hea, Muang, Chiang Mai 50100, Thailand

³Department of Industrial Chemistry, Faculty of Science, Chiang Mai University, Muang, Chiang Mai 50200, Thailand

Received 21 March 2007; accepted 22 July 2007

DOI 10.1002/app.27103

Published online 11 September 2007 in Wiley InterScience (www.interscience.wiley.com).

ABSTRACT: In this research, the effect of crystalline fraction of polypropylene (PP) on cell nucleation behavior was overcome by an introduction of solvent-plasticized step to the microcellular foaming in a solid-state batch-foaming process. Utilizing the plasticization performance of the solvent facilitated the PP to be foamed at the temperatures lower than its melting point with the dramatic development in the cellular morphology of the final foams. In consequence of the heterogeneous cell nucleation sites induction and the crystal-

line loss, which were induced by solvent, a high cell density (i.e., 10^9 – 10^{10} cells/cm³) was promoted without the cell sacrificing at the elevated temperatures (155 and 165°C) and favorable PP microcellular foams were accomplished. © 2007 Wiley Periodicals, Inc. *J Appl Polym Sci* 107: 63–70, 2008

Key words: polypropylene (PP); polypropylene foam; solvent plasticization; batch-foaming process; microcellular foam; morphology; nucleation; processing; swelling

INTRODUCTION

Microcellular foams are classified as a group of porous plastic materials that exhibit a very small bubble size (less than 50 μm) and with the cell density in excess of 100 million bubbles/cm³.¹ This interior structure of these materials influences the density reduction and the final foam properties. In addition, the use of these materials can reduce the consumption quantity of their raw material and cost-produced plastic parts without compromising on the mechanical properties. Because of the many advantages of microcellular foams, they have been introduced in many innovative industrial applications such as lightweight and high-strength automotive parts, packaging and aerospace industries, etc.^{2–4} To create the cellular structure in the polymeric matrix, the driving force for the activation of cell nucleation sites is basically induced by the thermodynamic instability phenomena. For a batch-foaming process, a solid polymer is exposed to an inert gas under high pressure^{5–11} in a pressure vessel after a sufficiently long time by means of the polymer becoming supersaturated with gas. Then the polymer/gas sys-

tem is removed from the pressure vessel and heated to the rubbery state⁹ to acquire as much amorphous region as possible. In this condition, the polymer exhibits a volume expansion and a large density of nuclei.^{5–11} The earlier studies in microcellular plastics field were mainly focused on the production of amorphous polymers such as poly(methyl methacrylate) (PMMA), polycarbonate, poly(vinyl chloride), and polystyrene.^{3,5,9,11–13} Because of the difficulties in controlling the cell nucleation of semicrystalline polymer foams such as high-density polyethylene (HDPE), polybutylene, polypropylene (PP), and poly(ethylene terephthalate),^{6–8,10} the study of these polymers was very challenging compared with that of amorphous polymers. The batch-foaming process of semicrystalline polymers was strongly dependent on their crystal morphology and the degree of crystallinity.^{6,7,14–17} Namely, the crystalline fraction of the polymer was a critical factor in the microcellular foaming process.^{7,14} Colton¹⁸ discussed that the crystalline phase was a form of stiff region in the polymer matrix. It inhibited the gas solubility in the matrix. Therefore, to enhance the gas solubility in the stiffness phase, the process required a high foaming temperature; close to its melting point to soften the matrix and reduce the surface tension of polymer/gas system.^{18,19} Moreover, the crystallinity and morphology of semicrystalline can be modified by controlling the cooling rate of polymer melt^{6,7,20} and blending or contamination of another phase (impurity or additive) in the matrix.^{15,16,21–23} The cell

Correspondence to: J. Pumchusak (jantra.t@chiangmai.ac.th).

Contract grant sponsors: Royal Thai Government and Graduate School of Chiang Mai University.

TABLE I
Properties of Raw Polypropylene Pellets

Resin properties	EP380T SW-844*
Melt flow rate (dg/min)	44
Density (g/cm ³)	0.9
Tensile strength at yield (MPa)	24
Melting temperature (°C)	167
Crystallinity (%)	36.9

morphology of blended foams was significantly improved compared with that of pure foams because of the presence of the dispersed phase generated in the heterogeneous nucleation sites in the matrix.²⁰ Rachtanapun et al.^{15–17} supported the influence of the blending of HDPE with PP that dramatically changed the crystalline morphology of polymer samples through the interfacial regions of the immiscible HDPE/PP blends, which served a lower activation energy for cell nucleation. However, the cell morphology gain of the blend samples was dependent on the blend composition.^{15–17} In addition, the stiffness effect of the polymer on foaming can be suppressed by the plasticization of some additives such as gas¹¹ or solvent²⁴, which is found in the continuous process of foaming as the formation of polymer/gas solution.²⁵

This research was motivated to generate the microcellular structure in PP matrix through the solid-state foaming process. The solubility parameter of chloroform is close to that of PP^{26–28}; therefore, it was selected to be used as a feasible additive to win over the effect of polymer crystallinity, and also it was expected to facilitate the development of microcellular foamed structure and foaming approach. Consequently, the chloroform-plasticized procedure was introduced in the foaming method before the gas saturation step. The effects of chloroform and processing condition on properties of foamed PP samples and cell morphology were investigated.

EXPERIMENTAL

Materials

PP polymer (Moplen EP380T SW-844), which was kindly supplied by HMC Polymers, Rayong, Thailand, was used to study the foaming. Its properties were listed in Table I. The original melting point and crystalline fraction of the polymer pellets were measured using differential scanning calorimeter [(DSC), DSC 550, Instrument Specialists] in the range of 25–200°C and at the heating rate of 10°C/min to survey the processing temperature for sample preparation and foaming process. Chloroform with 99.8% purity was used as a solvent in the solvent swelling step. Commercial grade (99.5% purity) of carbon

dioxide was used as blowing agent in the gas saturation step.

Sample preparation

Polymer pellets were preformed into 0.05-cm-thick sheets by compression molding machine (Lab Tech Engineering, Thailand) under a high pressure of 7.0 MPa at 185°C for 5 min, and the sample was cooled down at room temperature for 3 min. The sheet samples were cut into two different dimensional types (Type I: 1.25 cm × 2.54 cm and Type II: 1.25 cm × 7.00 cm). Type I samples were used to determine time requirements in the solvent saturation and the gas saturation steps, while Type II samples were used as the specimen in the foaming process. To transfer the Type I samples easily to the balance, they were cut into smaller sizes. Both types I and II samples were prepared in the thickness of 0.05 cm.

Determination of saturation time of chloroform absorption in PP

This procedure was introduced to estimate the saturated time for swelling the polymer samples with solvent. Erdogan and Pekcan²⁹ used chloroform as a swelling agent in the *in situ* swelling experiment for PMMA. In general, a similar or an equivalent solubility parameter of a solvent and a polymer is necessary for polymer–solvent system.^{26,27} Therefore, chloroform was selected to use as a solvent to swell the polymer samples in the lab scale experiment. The solubility parameters of chloroform and PP are 17.9 and 19.0 MPa^{0.5}, respectively.²⁸ The swelling behavior of the polymer was investigated by measurement of the mass uptake of solvent on the polymer samples and this experiment was performed as the determination of degree of swelling.³⁰ Ten replicates of Type I samples were immersed in chloroform at various periods of time. The mass uptakes of the samples were measured immediately at 25°C ± 2°C (lower than the boiling point of chloroform)³¹ after they were taken out of the solvent bottle, and the solvent on the sample surfaces was wiped out. The plot of the penetrated solvent quantity and experimental time revealed the saturated time as shown in Figure 1.

Investigation of chloroform performance on the crystallinity of PP

The effect of chloroform performance on the polymer crystallinity was investigated by the thermal analysis of PP polymer using DSC. Preformed sheet sample was denoted as “non-solvent sample” and the other was designated as “chloroform-swollen

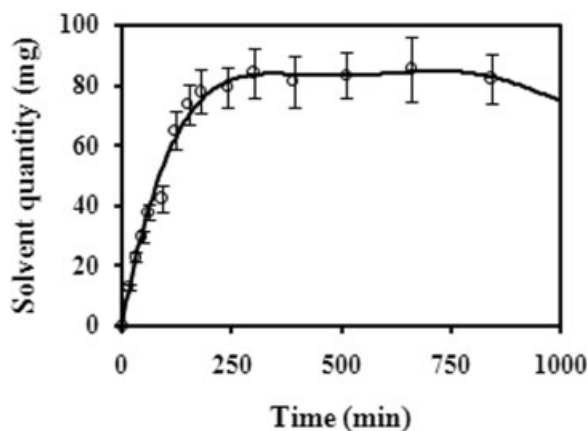


Figure 1 Solvent absorption curve of chloroform-swollen PP sheet at ambient condition.

sample." Four replicates of both samples were randomly collected (3–5 mg). The sample was heated up from room temperature to 200°C at 10°C/min under N₂ atmosphere. The comparison of the DSC thermograms of both samples was elucidated as the DSC thermograms as shown in Figure 2. The crystalline fractions of both samples were calculated based on 209 J/g of heat of fusion for PP³² and they were listed in (Table II).

Saturation time of CO₂ in PP determination

The objective of this experiment was to study the absorption behavior of the blowing agent (CO₂) in the polymer matrix. In this step, three replicates of Type I samples were pressurized in a pressure vessel with 5.5 MPa of CO₂ at room temperature for various periods of time. Then samples were taken out and the weight gain of the samples was measured using the balance at 25°C ± 2°C and immediately recorded. The determination of gas saturation time

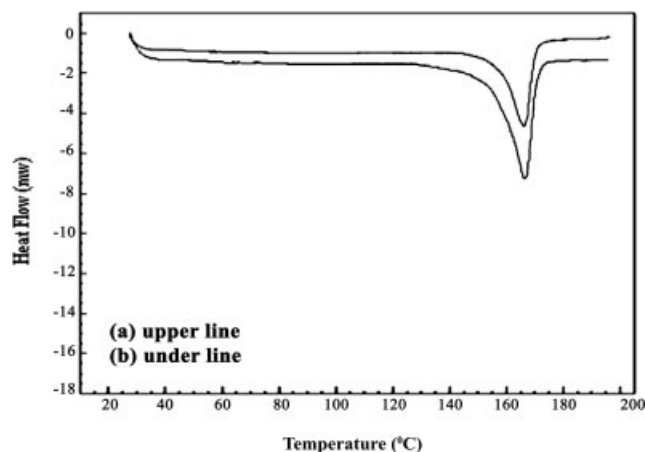


Figure 2 DSC thermograms of (a) chloroform-swollen sheet and (b) nonsolvent sheet at 25–200°C and the heating rate of 10°C/min under N₂ atmosphere.

TABLE II
Thermal Properties and Crystallinity (%) of Nonsolvent and Chloroform-Swollen Samples

Condition	Onset temperature (°C)	T _m (°C)	Heat of fusion (J/g)	Crystallinity
Nonsolvent samples	149	166	95.9	45.9
	151	167	92.6	44.3
	150	167	91.8	43.9
	152	166	90.2	43.2
Average	150 ± 1.3	166 ± 0.6	92.6 ± 2.4	44.3 ± 1.1
Chloroform-swollen samples	148	163	74.9	35.8
	153	165	77.9	37.2
	152	165	74.3	35.5
	154	166	76.3	36.5
Average	152 ± 2.6	165 ± 1.3	75.9 ± 1.6	36.3 ± 0.8

is a widely well-known method as described in many research papers.^{7,15,33,34}

The remaining amount of gas in the polymer at time and the amount of gas at equilibrium state were M_t and M_∞ , respectively. The diffusivity (D) for absorption was calculated using Eq. (1).^{6,7,23}

$$\frac{M_t}{M_\infty} = 4(D/\pi)^{0.5}(t^{0.5}/L) \quad (1)$$

where, t and L were assigned as the absorption time (s) and sample thickness (cm), respectively. A plot of M_t/M_∞ as a function of $t^{0.5}/L$ yields essentially a straight line (for the initial period of test) with a slope of $4(D/\pi)^{0.5}$, which is readily solved for D . Figure 3 shows a plateau line and the saturation time was received from this time period.

Foaming experiment

In this experiment, Type II samples were used and they were divided into two sets; the first set was processed as controlled sample (nonsolvent sample) and the other was immersed into chloroform for 8 h (considering solvent-saturated time in Fig. 1) at ambient

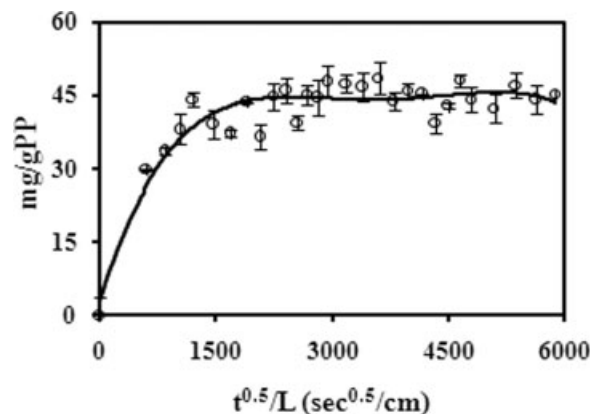


Figure 3 Gas absorption curve of CO₂ in PP sheet at 5.5 MPa and 25°C.

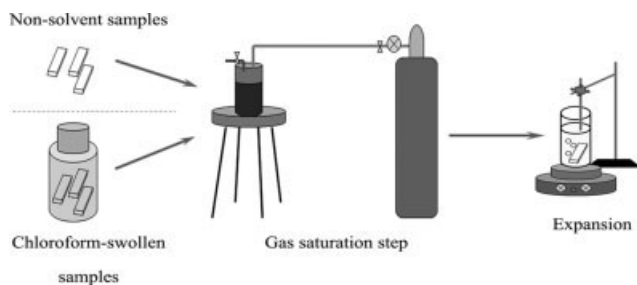


Figure 4 Experimental set up for a solid-state batch-foaming process.

condition, which was denoted as chloroform-swollen sample. After that both samples were pressurized in a pressure vessel with CO_2 at 25°C and 5.5 MPa for 8 h (considering gas-saturated time in Fig. 3). The samples were removed from the pressure vessel and expanded in hot glycerin oil at four different temperatures (50, 100, 155, and 165°C) for 3 s. In the case of foaming at room temperature (25°C), the saturated samples were allowed to foam in the atmosphere. After expansion, the foamed samples were suddenly quenched in a media (ethanol/distilled water = 1/1) to suppress the cell coalescence and the residue of glycerin oil was washed. All steps in the foaming process were set up as shown in Figure 4. The final foamed products of chloroform-swollen samples were studied comparatively with that of nonsolvent samples in terms of the density reduction, void fraction, cell density, and average cell size correlated to the processing condition as following.

Characterization of final foams

The effects of chloroform and processing condition on the final foam characteristics were investigated by means of percentage of density reduction, void fraction, cell population density, and cell size. The density was determined by water displacement method (ASTM D-792)^{3,35} and the void fraction (V_f) was calculated on the basis of the ratio of the bulk density of foamed sample (ρ_f) and unfoamed samples (ρ) as in eq. (2).^{3,5,15,35}

$$V_f = 1 - \frac{\rho_f}{\rho} \quad (2)$$

The cellular structure of foamed samples was investigated using scanning electron microscopy [(SEM), JEOL JSM-5910 LV] micrographs. The cell density (N_0) of final foams was calculated using eq. (3).^{3,5,35}

$$N_0 = \left[\frac{nM^2}{A} \right]^{3/2} \times \left[\frac{1}{1 - V_f} \right] \quad (3)$$

where n is the number of bubbles in the micrograph, and A and M are the area and the magnification factor of the micrograph, respectively. In this article, A and M used for cell density and cell size determination were 344 cm^2 and $500\times$, respectively. From eqs.

(2) and (3), the average cell size (d) can be determined as eq. (4).³⁵

$$d = \sqrt[3]{\frac{6V_f}{\pi N_0(1 - V_f)}} \quad (4)$$

RESULTS AND DISCUSSION

Saturated time for chloroform absorption in PP

The saturated time for solvent penetration into the polymer matrix was determined from solvent absorption curve through the solvent-swelling experiment as shown in Figure 1. At the initial state, the solubility was dramatically increased as time increased, but it was tended to level off after 5 h. The steady state (in the range of 6–12 h) of the curve revealed the time required for chloroform to plasticize the polymer. In this experiment, 8 h of saturation time was selected to perform on the solvent-swelling step. It was found that for more than 12 h of sample immersion in chloroform, partly dissolution of the matrix into the solvent occurred, which yielded the weight reduction of the matrix.

Effect of chloroform on the crystalline fraction of PP

The foaming process of semicrystalline polymer usually requires a high temperature near its melting point.¹⁸ Moreover, the thermal property investigation of raw plastic material used was necessary as a basic data for polymer manufacture. Therefore, thermal properties of PP were determined by DSC to use these values as basic information in the foaming process. The melting temperature (T_m) of the original polymer pellets was 167°C with $\approx 37\%$ of crystalline fraction. As the results in Figure 2 and Table II show, the crystallinity of nonsolvent sample was increased to $\approx 44\%$ because of the secondary crystallization (heat annealing)³⁶ in sample preparation step. After the samples were softened by chloroform, the crystalline fraction was significantly reduced to $\approx 36\%$ of the smaller amount of heat of fusion at the melting temperature of the sample (76.3 J/g); this is because chloroform can act as a plasticizer to decrease the order of polymer chain fold as it was reported for the blending effect^{15–17} or the performance of fast cooling rate in quenching step.^{6,7} As the influence of heterogeneous sites was induced to facilitate the foaming ability of PP resin by using some additives or contamination of secondary phase as well as blending of another component into the main polymer matrix, this made the matrix to be soft to contribute to the increase of gas solubility. Since the stiffness of the polymer was reduced as the interfacial regions occurred, the bubbles with micro-

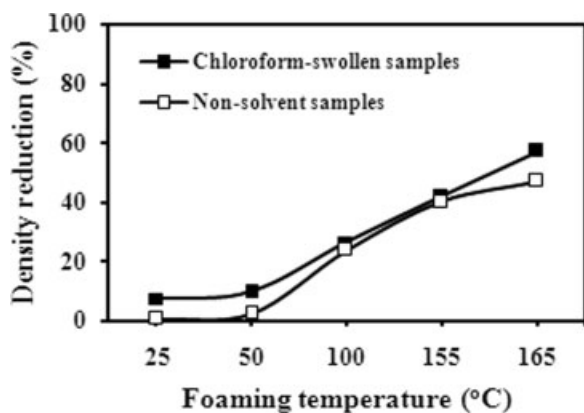


Figure 5 Density reduction of foamed samples at various temperatures.

cellular characteristics could be nucleated.^{15–17,20–23} Therefore, chloroform was selected to increase the stiffness loss in PP resin, and the performance of this solvent has been investigated. The thermal properties and the reduction of crystallinity of nonsolvent and chloroform-swollen samples were shown in Figure 2 and Table II. The crystalline fraction of chloroform-swollen samples was lower than that of nonsolvent samples by about 18%. Moreover, the melting temperature of chloroform-swollen samples was slightly lower than that of nonsolvent samples. This evidenced that chloroform can not only act as a plasticizer to swell the polymer but it was also effective enough to lower the order of polymer chain fold; therefore, chloroform eased the gas absorption and foaming of PP.

Saturated time for CO₂ absorption in PP

It is known that the blowing agent (CO₂ gas) absorption of polymers is different; therefore, the CO₂ absorption of PP was determined in order to gain the gas saturation time. This period of time would be applied to the gas saturation step prior to the foaming process.^{5–11,15,16,23} The CO₂ solubility behavior in PP matrix was shown in Figure 3 as the gas absorption curve. This figure showed the initial linear relationship between M^t and $t^{0.5}/L$. After the gas solubility was eventually converged to a steady state, it then represented the constancy of gas solubility in the polymer.^{6,7,23} This plateau revealed the gas saturation time, which was about 8 h. Therefore, the samples were exposed to CO₂ gas for 8 h before foaming process.

Effect of chloroform and processing condition on density and void fraction

After the investigation of physical properties and morphology of final foams, the samples (nonsolvent

and chloroform-swollen samples) possessed significantly different results. The experimental results showed the temperature dependence of the density reduction and the void fraction. They increased when the foaming temperature increased because the dissolved gas can easily be diffused into the polymer matrix at the elevated temperature.³⁵ The research of Rachtanapun et al.^{16,17} revealed that the cell morphology of pure PP samples was developed when the foaming temperature was increased to 175°C. At low temperatures (i.e., 135 or 160°C), the cellular structure could not be located in the polymer matrix because the temperature was lower than the melting point of PP. In spite of this, foaming the samples above the melting temperature potentially improved the morphology and void fraction in the matrix; however, the cellular structure was not uniform. This is because the crystallinity effect and the hindrance of polymer sheet thickness could not contribute to the uniform cell nucleation and uniform heat transfer through the sample. Therefore, a large cell size was only nucleated on the surface area of the sample, whereas the center of sample was not foamed. However, it was found that microcellular structure was developed in the subsurface. From the evidence of an introduction of the secondary phase into PP matrix it was possible to increase crystallinity loss in the PP regions due to a low viscosity of another phase, resulting in too soft material, which was too soft to maintain the microstructure.^{16,17} Our experimental results showed that utilizing the chloroform-swelling step before the gas saturation procedure could facilitate the reduction of foamed density and enhance the void fraction as shown in Figs. 5 and 6, respectively. Chloroform acted as a plasticizer, which located between polymer chains and made the chain far apart. Therefore, the reduction of crystallinity was observed as shown in Table II. Figures 5 and 6 show the similar tendency of density reduction and void fraction with respect to the foam-

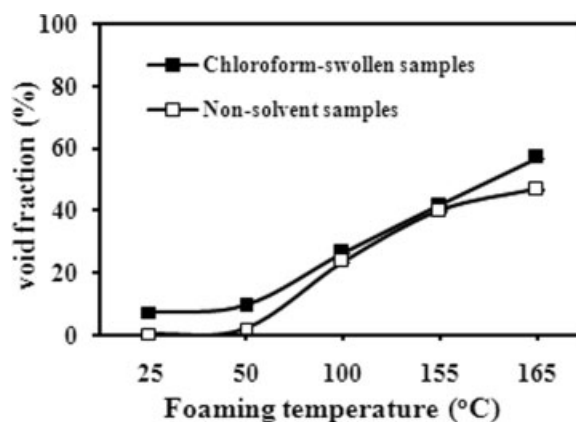


Figure 6 Void fraction of foamed samples at various temperatures.

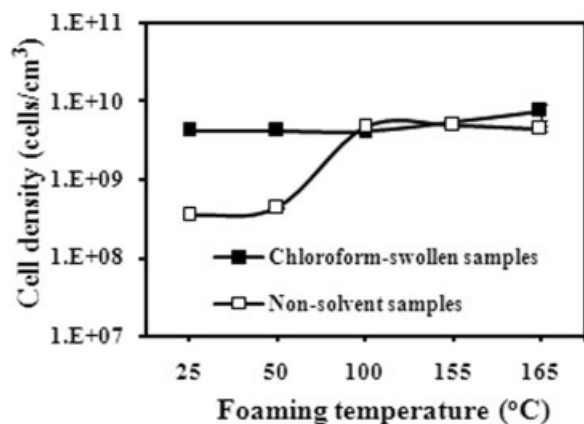


Figure 7 Cell density of foamed samples at various temperatures.

ing temperature, respectively. For foaming at 25 and 50°C, the density reduction and the void fraction of chloroform-swollen samples were 7–10%. But they were only achieved \approx 3–5% when foaming the samples without chloroform. Foaming at temperatures higher than 100°C showed theoretically the increase in the density reduction and the void fraction as the temperature increased and they were higher than those of foaming at low temperatures (25 and 50 °C) \approx 76–93%. In addition, chloroform-swollen samples provided an increase of density reduction and void fraction at all foaming temperatures comparatively with those of nonsolvent samples. It can be said that a high void fraction and a high density reduction of the final cellular structure would be achieved without the deformation of polymer and cell sacrifice at high foaming temperature when including of the solvent swelling step to the foaming procedure. It can be seen that including solvent-swelling step was superior than blending other phase into PP^{16,17} in terms of foaming. Because the accomplishment of blending with the same amount of void fraction had to be processed at higher foaming temperature (i.e., 160 or 175°C) for a longer period of time, our studied method gave the same quality of foamed product at a lower foaming temperature (at the ambient condition). Moreover, the blended ratio of all components was a crucial factor to contribute to the nucleation area for the uniformity of fine-celled foams, especially in the case of blending.

Effect of chloroform and processing condition on cell morphology

It is well known that it was very difficult to receive a uniform microcellular structure in the solid-state foaming process when a polymer had a high crystalline fraction, which inhibited the gas absorption in the matrix.^{6,14,18} However, the stiffness phase of the polymer could be modified by various methods as

previously mentioned.^{16–18} After modification of the polymer matrix, the crystalline phase was shifted to amorphous phase resulting in the reduction in crystalline fraction. A uniform cell distribution with a large number of cell nucleation was then promoted due to the ease of gas solubility in amorphous regions.^{14–16,21–24} It was reported that for HDPE/PP blend, even at the foaming temperature above its melting point, the cellular structure was developed only at the surface but not at the center.^{16,17} However, the uniform cell distribution and microcellular structure could develop when chloroform was used to overcome the hindrance of crystallinity in PP microcellular foaming as the results of this research. The cell morphology of final foams was investigated using SEM micrograph; cell density and average cell size of all samples increased as the foaming temperature increased and they exhibited the cell density in the range of 10^8 – 10^{10} cells/cm³ with a small cell size of 3–8 μ m. In the case of chloroform-swollen samples, the uniform distribution of micro-cell number was increased regardless of the elevated foaming temperature; a high cell density ($\approx 10^{10}$ cells/cm³) could be obtained by using the temperature only at 25 or 50°C. On the other hand, to receive the same amount of cell density for the case of foaming without the solvent-swelling step the samples required a high foaming temperature (i.e., 100–165°C) to generate a high density of nuclei. This is because the crystallinity of the polymer inhibited the gas solubility in the matrix^{6,14,18} but cell size of samples seemed to be bigger than those of chloroform-swollen samples as shown in Figures 7 and 8. Moreover, the cell-to-cell diffusion of blowing agent was accelerated easily under a high temperature. Since the blowing agent diffused through the cell wall of the adjacent cells, the cells coalescence phenomena resulted in larger cells in the final foams³⁵ as shown in Figure 9(c–e). Likewise allowing the samples to expose with chloro-

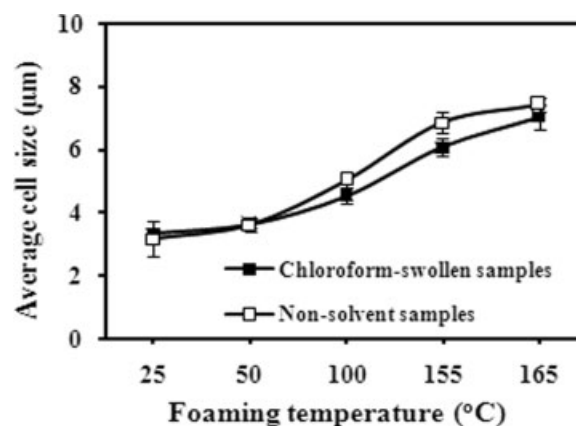


Figure 8 Average cell size of foamed samples at various temperatures.

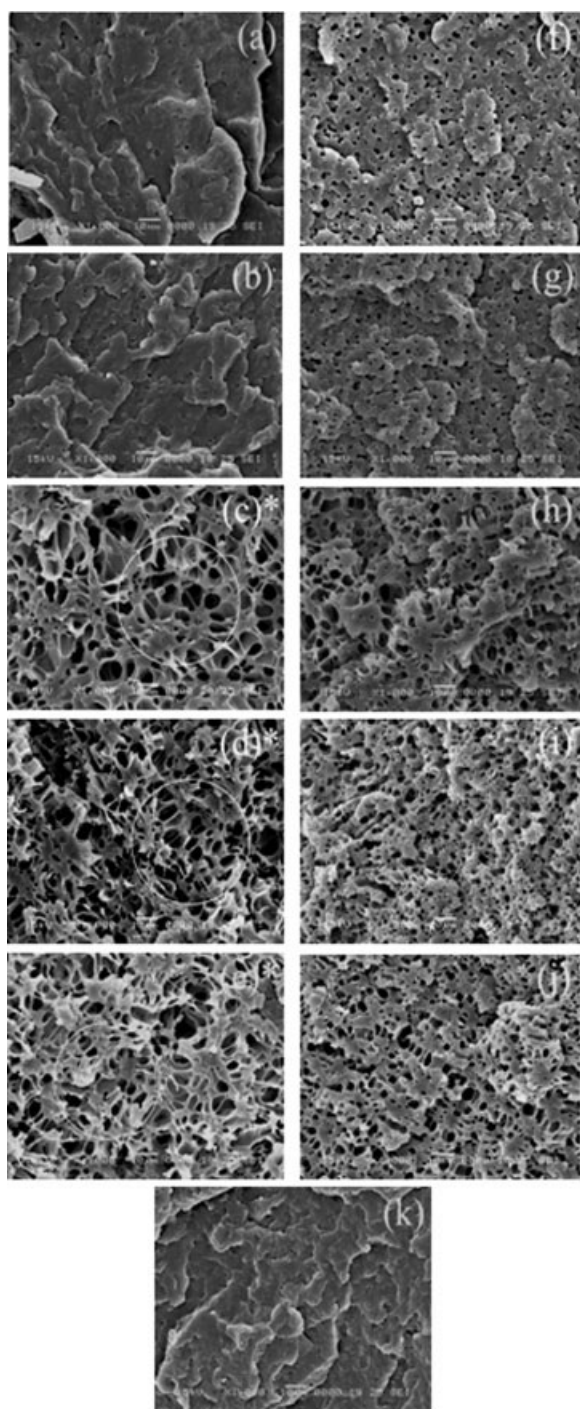


Figure 9 (a–e) SEM images of nonsolvent foamed samples at foaming temperature 25, 50, 100, 155, and 165 °C, respectively; (f–j) SEM images of chloroform-swollen samples at foaming temperatures 25, 50, 100, 155, and 165 °C, respectively; (k) preformed sample. The magnification of all SEM images is $\times 1000$. *The circle areas in these figures indicate the interconnected cellular structure.

form before gas saturation step, fine cell size (in the range of 3–8 μm) and uniformity of isolated foams were successfully achieved for all foaming temperatures as shown in Figure 9(f–j). Though chloroform-swollen samples seemed to exhibit some big bubbles

at the temperatures in the range of 100–165 °C, the interconnected cells did not locate in the polymer matrix as the case of nonsolvent sample (noticeable circle areas) as shown in Figure 9(c–e). It was discussed that an introduction of chloroform-swelling step in the foaming procedure was very effective to create a large cell-population density and fine-celled PP foams due to the effect of plasticization and the heterogeneous nucleation site generation of dissolved chloroform in the matrix. In addition, a high density of fine cell without the cell coalescence could be achieved regardless the foaming temperature.

CONCLUSIONS

In this research, the influence of the stiffness phase due to the crystalline fraction of PP was a critical point to encourage improving the processability of PP microcellular foam. Chloroform, an organic solvent in the *in situ* swelling experiment, was selected to swell the polymer matrix before the gas saturation step to enhance the stiffness loss in the matrix due to the comparable solubility parameter of PP and chloroform. The crystallinity change evidenced the significant performance of chloroform to allow a high content of gas to be absorbed into the polymer matrix during the process which resulted in a high density of nuclei. To achieve the same amount of cell density, nonsolvent samples required a high foaming temperature (near the melting point of the matrix) and the cell coalescence phenomena still appeared in the products. Therefore, an introduction of solvent plasticization using chloroform as a plasticizer was a profit to generate the microcellular structure in PP matrix for the solid-state batch-foaming process as an accomplishment of a high cell density and very fine-celled PP foam. Furthermore, the resulting microcellular foams could be foamed at the ambient by using our strategy. In addition, the researcher has planned to further publish the effect of solvent plasticization on the mechanical properties of the microcellular PP foams in a separate article.

HMC polymers, Thailand, is appreciated for their generous supply of PP polymer for this research.

References

1. Suh, N. P. *Macro Symp* 2003, 201, 187.
2. Baldwin, D. F.; Tate, D. E.; Park, C. B.; Cha, S. W.; Suh, N. P. *Seikei-Kakou* 1994, 6, 187.
3. Matuana, L. M.; Park, C. B.; Balatinecz, J. J. *Cell Polym* 1998, 17, 1.
4. Klemptner, D.; Sendjarevic, V. *Handbook of Polymeric Foams and Foam Technology*, 2nd ed.; Hanser: Munich, 2004.
5. Matuana, L. M.; Park, C. B.; Balatinecz, J. J. *J Cell Plast* 1996, 32, 449.

6. Doroudiani, S.; Park, C. B.; Kortschot, M. T.; Cheung, L. K. SPE ANTEC Tech Pap 1995, 41, 2183.
7. Doroudiani, S.; Park, C. B.; Kortschot, M. T. Polym Eng Sci 1996, 36, 2645.
8. Kumar, V.; Stolarczuk, P. J. SPE ANTEC Tech Pap 1996, 1894.
9. Holl, M. R.; Kumar, V.; Ma, M.; Kwapisz, R. R. SPE ANTEC Tech Pap 1996, 1908.
10. Kumar, V.; Eddy, S.; Murray, R. SPE ANTEC Tech Pap 1996, 1920.
11. Holl, M. R.; Kumar, V.; Garbini, J. L.; Murray, W. R. J Mater Sci 1999, 34, 637.
12. Geol, S. K.; Beckman, E. J. Polym Eng Sci 1994, 34, 1137.
13. Geol, S. K.; Beckman, E. J. Polym Eng Sci 1995, 34, 1148.
14. Maier, C.; Calafut, T. Polypropylene: The Definitive User's Guide and Databook; Plastics Design Library: New York, 1998; Chapter 8.
15. Rachtanapun, P.; Selke, S. E. M.; Matuana, L. M. J Appl Polym Sci 2003, 88, 2842.
16. Rachtanapun, P.; Selke, S. E. M.; Matuana, L. M. Polym Eng Sci 2004, 44, 1551.
17. Rachtanapun, P.; Selke, S. E. M.; Matuana, L. M. J Appl Polym Sci 2004, 93, 364.
18. Colton, J. S. Mater Manu Proc 1989, 4, 253.
19. Baldwin, D. F.; Park, C. B.; Suh, N. P. Polym Eng Sci 1996, 36, 1446.
20. Ke, B. J Polym Sci 1962, 61, 47.
21. Noel, O. F.; Carley, J. F. Polym Eng Sci 1984, 24, 488.
22. Teh, J. W.; Blom, H. P.; Rudin, A. Polymer 1994, 35, 1680.
23. Doroudiani, S.; Park, C. B.; Kortschot, M. T. SPE ANTEC Tech Pap 1996, 1914.
24. Doolite, A. K. J Polym Sci 1947, 2, 121.
25. Baldwin, D. F.; Tate, D. E.; Park, C. B.; Cha, S. W.; Suh, N. P. Seikei-Kakou 1994, 6, 245.
26. 2.0 Literature Review (2005) [Online]. Available at <http://scholar.lib.vt.edu/theses/available/etd-62398-82953/unrestricted/Chapter2.PDF> (April 2005).
27. Perkins, J. L. Solvent-Polymer Interactions; American Industrial Hygiene Association; Akron: Ohio, 1998.
28. Brandup, J.; Immergut, E. H.; Grulke, E. Polymer Handbook, 4th ed.; Wiley: New York, 1999.
29. Erdogan, M.; Pekcan, O. Int J Photoenergy 2005, 7, 37.
30. Experimental 5: Swelling and Solute Transport Properties of Hydrogels [2007, Online]. Available at <http://ocw.mit.edu/NR/rdonlyres/Chemical-Engineering/10-467Fall-2005/F0D4A260-9BDE-4892-B1FC-0B60101C90D9/0/5.pdf> (May 2007).
31. Wikipedia. The Free Encyclopedia, Chloroform [2007, Online]. Available at <http://en.wikipedia.org/wiki/Chloroform> (May 2007).
32. Wunderlich, B. Macromolecular Physics: Crystal Structure, Morphology, Defects; Academic Press: New York, 1973.
33. Baldwin, D. F.; Suh, N. P.; Shimbo, M. Cell Polym ASME 1992, 38, 109.
34. Baldwin, D. F.; Park, C. B.; Suh, N. P. Polym Eng Sci 1996, 36, 1437.
35. Matuana, L. M.; Park, C. B.; Balatinez, J. J. Polym Eng Sci 1997, 37(7), 1137.
36. Keller, A. Pure Appl Chem 1992, 64, 193-204.